Amino acid substitutions in ribosomal protein RpsU enable switching between high fitness and multiple-stress resistance in *Listeria monocytogenes*

Jeroen Koomen [a], Linda Huijboom [a], Xuchuan Ma [a], Marcel H. Tempelaars [a], Sjef Boeren [b], Marcel H. Zwietering [a], Heidy M.W. den Besten [a], Tjakko Abee [a,*]

[a] *Food Microbiology, Wageningen University and Research, the Netherlands, P.O. Box 17, 6700 AA Wageningen, the Netherlands*
[b] *Laboratory of Biochemistry, Wageningen University and Research, the Netherlands*

ARTICLE INFO

ABSTRACT

Microbial population heterogeneity contributes to differences in stress response between individual cells in a population, and can lead to the selection of genetically stable variants with increased stress resistance. We previously provided evidence that the multiple-stress resistant *Listeria monocytogenes* LO28 variant 15, carries a point mutation in the *rpsU* gene, resulting in an arginine-proline substitution in ribosomal protein RpsU (RpsU$^{17\text{Arg-Pro}}$). Here, we investigated the trade-off between general stress sigma factor SigB-mediated stress resistance and fitness in variant 15 using experimental evolution. By selecting for higher fitness in two parallel evolving cultures, we identified two evolved variants: 15EV1 and 15EV2. Whole genome sequencing and SNP analysis showed that both parallel lines mutated in the same codon in *rpsU* as the original mutation resulting in RpsU$^{17\text{Pro-His}}$ (15EV1) and RpsU$^{17\text{Pro-Thr}}$ (15EV2). Using a combined phenotyping and proteomics approach, we assessed the resistance of the evolved variants to both heat and acid stress, and found that in both lines reversion to WT-like fitness also resulted in WT-like stress sensitivity. Proteome analysis of *L. monocytogenes* LO28 WT, variant 15, 15EV1, and 15EV2 revealed high level expression of SigB regulon members only in variant 15, whereas protein profiles of both evolved variants were highly similar to that of the LO28 WT. Experiments with constructed RpsU$^{17\text{Arg-Pro}}$ mutants in *L. monocytogenes* LO28 and EGDe, and RpsU$^{17\text{Arg-His}}$ and RpsU$^{17\text{Arg-Thr}}$ in LO28, confirmed that single amino acid substitutions in RpsU enable switching between multiple-stress resistant and high fitness states in *L. monocytogenes*.

1. Introduction

Listeria monocytogenes is a foodborne pathogen that is ubiquitously present in the environment, and can cause the rare but severe disease listeriosis (Lecuit, 2007; Radoshevich and Cossart, 2018; Vázquez-Boland et al., 2001). *L. monocytogenes* is considered a robust organism, since it can adapt to and survive a wide range of stress conditions such as low pH, low temperature and low water activity (a$_w$) (NicAogáin and O'Byrne, 2016).

The inherent heterogeneity of microbial populations is one of the factors that contribute to the ubiquitous nature of *L. monocytogenes* supporting its capacity to cope with environmental stresses during its transmission from the environment to the human gastro-intestinal tract. Notably, differences in stress response between individual cells of a population can lead to survival of a small fraction of the population when the population is subjected to lethal stresses such as heat or low

pH, leading to tailing of the inactivation curve. Tailing results in higher than expected numbers of cells surviving an inactivation treatment, either as transiently resistant subpopulations, or as genetically stable variants with increased stress resistance (Gollan et al., 2019; Karatzas et al., 2005; Metselaar et al., 2013; Van Boeijen et al., 2008).

Previously, Metselaar et al. (2015) combined phenotypic clustering of a collection of stable stress resistant *L. monocytogenes* variants, based on reduced growth rate and increased resistance against acid, heat, high hydrostatic pressure (HHP), and benzalkonium chloride, with a whole genome sequencing and Structural Variation (SV) analysis. This analysis showed that 11 of the 23 selected variants with a shared phenotype had a mutation in the ribosomal *rpsU* gene locus encoding S30 ribosomal protein RpsU (small ribosomal protein 21) (Metselaar et al., 2015). Subsequent work focused on two of the variants; variant 14, with a large deletion that spans the whole *rpsU* gene, as well as *yqeY* and half of *phoH*; and variant 15, with a single point mutation in *rpsU* that resulted in an

amino acid substitution from arginine to proline in the RpsU protein, RpsU[17Arg-Pro] (Koomen et al., 2018). Comparative analysis of gene expression profiles and phenotypes of *L. monocytogenes* LO28 wildtype (WT) and multiple-stress resistant variants 14 and 15, revealed upregulation of 116 genes with a major contribution of genes controlled by the alternative stress sigma factor SigB (Koomen et al., 2018). Activation of SigB is controlled by the so-called stressosome, a cytoplasmic complex that relays a range of stress signals and activates the sigma B regulon providing multiple-stress resistance (Guldimann et al., 2016; NicAogáin and O'Byrne, 2016; Radoshevich and Cossart, 2018). Next to stress defence activation, the multiple-stress resistant *L. monocytogenes* variants 14 and 15 had increased glycerol metabolic capacity and reduced expression of flagella (Koomen et al., 2018). Modelling and validation of the ecological behaviour of *L. monocytogenes* WT and stress resistant variants 14 and 15 led to the hypothesis that multiple stress resistance could contribute to performance and persistence in the food chain, which, in combination with the conceivable higher survival of acidic conditions in the stomach, could result in a higher exposure and risk of disease (Abee et al., 2016; Metselaar et al., 2016). An additional factor contributing to increased risk following the initial selection of multiple stress resistant variants (Abee et al., 2016) could be the subsequent selection of other variants that originate from the ancestor variant and have increased fitness and loss of the stress resistant phenotype.

In the current study, we addressed this issue and subjected *L. monocytogenes* LO28 variant 15, with its single point mutation in *rpsU*, resulting in RpsU[17Arg-Pro], to an experimental evolution regime where we selected for higher fitness, defined as an increased maximum specific growth rate (μ_{max}), when compared to the ancestor variant 15. Subsequent genotyping and phenotyping of evolved variants has provided insights in *L. monocytogenes* switching between high fitness-low stress resistance, and low fitness-high stress resistance.

2. Materials and methods

2.1. Bacterial strains and culture conditions

For genotypic, proteomic and phenotypic analysis, *L. monocytogenes* LO28 wild type (WT) strain (Wageningen Food & Biobased Research, The Netherlands), stress resistant ancestor variant 15 (Koomen et al., 2018; Metselaar et al., 2013), and evolved variants (this study) were used. All bacterial cultures were grown as described elsewhere (Metselaar et al., 2013). Briefly, cells from −80 °C stocks were grown at 30 °C for 48 h on brain heart infusion (BHI, Oxoid, Ltd., Basingstoke, England) agar (1.5% [*w/w*], bacteriological agar no. 1 Oxoid) plates. A single colony was used to inoculate 20 mL of BHI broth in a 100 mL Erlenmeyer flask. After overnight (ON, 18–22 h) culturing at 30 °C under shaking at 160 rpm, (Innova 42, New Brunswick Scientific, Edison, NJ) 0.5% (*v/v*) inoculum was added to fresh BHI broth. Cells were grown under shaking at 160 rpm in BHI at 30 °C until the late-exponential growth phase (OD600 = 0.4–0.5).

2.2. Experimental evolution

Experimental evolution was performed by inoculating two parallel lines with 1% (*v/v*) of ON culture of *L. monocytogenes* LO28 variant 15, in 20 mL BHI in 100 mL Erlenmeyer flasks, resulting in approximately $1 * 10^{7.5}$ cfu/mL. The cultures were incubated for 24 h at 20 °C under continuous shaking at 160 rpm (Innova 42). For each parallel line, 28 consecutive transfers were made using 24 h-cultures and 1% (*v/v*) inoculum to inoculate fresh BHI. Each transfer allowed for a 2-log increase (~6.65 generations), and for 28 transfers this yields in total around 200 generations. From every second transfer, a 700 μL culture sample was taken, mixed with glycerol (Sigma-Aldrich, the Netherlands, 25% v/v final concentration), flash frozen in liquid nitrogen, and stored at −80 °C, resulting in 14 stocks. These stocks were revived by streaking on BHI agar plates, and a single colony was used to inoculate 20 mL of

BHI broth in a 100 mL Erlenmeyer flask. After ON culturing at 30 °C under shaking at 160 rpm, (Innova 42) the culture was diluted 100,000 times in fresh BHI broth, and 200 μL of culture was inoculated in duplicate in wells of a honeycomb plate. The plate was incubated in a Bioscreen C (Oy Growth Curves AB Ltd., Helsinki, Finland) at 30 °C and the respective growth curves were determined by measuring OD600 over time, using biological triplicates. The starting stocks, and the first stocks where a clear shift to WT-like growth was observed, i.e., stock number 8 for 15EV1 (after 16 daily transfers) and number 9 for 15EV2 (after 18 daily transfers), were streaked on BHI agar, and respective single colonies were selected to prepare −80 °C stocks of 15EV1 and 15EV2 and the ancestor variant 15. These stocks were used for whole genome sequencing and subsequent phenotyping experiments.

2.3. Estimation of μ_{max}

The maximum specific growth rate μ_{max} was determined for the two evolved strains (15EV1 and 15EV2), variant 15 and the LO28 WT strain. For that, ON cultures were diluted 1000 times in peptone physiological salt solution (PPS, Tritium Microbiologie B.V., the Netherlands), after which they were diluted another 100 times in BHI broth, resulting in a concentration of ~$4 * 10^4$ cfu/mL, which was confirmed by plating on BHI agar. The μ_{max} was estimated using the 2-fold dilution method, as described previously by (Biesta-Peters et al., 2010), which is based on the time-to-detection (TTD) of serially diluted cultures. Briefly, for each strain tested, a two-fold dilution series was made in duplicate from the first well to the fifth well, by mixing 200 μL of bacterial culture and 200 μL of fresh BHI in honeycomb plates. The plates were incubated in a Bioscreen C (Oy Growth Curves AB Ltd) at 30 °C with continuous shaking. The TTD was defined as the time at which a well reaches an OD600 value of 0.2. Data processing and estimation of the TTD was done in Microsoft Excel (Redmond, Washington, USA). The μ_{max} was calculated as the negative reciprocal slope of the linear regression between TTD and the natural logarithm of the initial bacterial concentration of the five wells for each culture, where μ_{max} equals ln(2)/generation time (i.e., $\mu_{max} = 1$ represents a generation (doubling) time of approximately 0.7 h, or 42 min). Three biologically independent experiments were performed to estimate the mean and standard deviation of μ_{max}.

2.4. Inactivation kinetics at low pH

Acid inactivation experiments were performed as described previously (Metselaar et al., 2013). Briefly, 100 mL of late-exponential phase culture was pelleted for 5 min at 2880 x *g* in a fixed-angle rotor (5804 R, Eppendorf). Pellets were washed in 10 mL BHI broth and pelleted again at 5 min at 2880 ×*g*. The pellet was resuspended in 1 mL PPS that was pre-warmed to 37 °C and adjusted to pH 3.0 using 10 M of HCl, and placed in a 100 mL Erlenmeyer flask in a shaking water bath at 37 °C. At different time intervals, samples were taken, decimally diluted in BHI broth and plated on BHI agar using an Eddy Jet spiral plater (Eddy Jet, IUL S.A.) Plates were incubated at 30 °C for 4–6 days to allow for full recovery of damaged cells. Combined data of at least three biologically independent experiments were used for analysis.

2.5. Inactivation kinetics at high temperature

Heat inactivation experiments were performed as described before (Metselaar et al., 2015). Briefly, 400 μL of late-exponential phase culture was added to 40 mL of fresh BHI broth that was pre-heated to 55 °C ± 0.3 °C. A separate Erlenmeyer with BHI at room temperature was used to determine the initial microbial concentration. Samples were taken after various timepoints and decimally diluted in PPS. Appropriate dilutions were plated on BHI agar using an Eddy Jet spiral plater (Eddy Jet, IUL S. A.) in duplicate. Combined data of at least 3 biologically independent experiments were used for analysis.

2.6. Proteomic analysis

Cultures of the LO28 WT, variant 15 and evolved 15EV1 and 15EV2 were grown as described in 2.1. For proteomic analysis, 2 mL of sample with OD_{600} of 0.4–0.5 was flash frozen in liquid nitrogen and stored until further use. Samples were thawed on ice and pelleted at 17,000 x *g*. Pellets were washed twice with 100 mM Tris (pH 8) to remove traces of BHI. Pellets were resuspended in 100 µL of 100 mM Tris (pH 8) and were sonicated three times for 30 s on ice to lyse the cells. Samples were prepared according to the filter assisted sample preparation protocol (FASP) (Wiśniewski et al., 2009) with the following steps: reduction with 15 mM dithiothreitol, alkylation with 20 mM acrylamide, and digestion with sequencing grade trypsin overnight. Each prepared peptide sample was analyzed by injecting (18 µL) into a nanoLC-MS/MS (Thermo nLC1000 connected to an LTQ-Orbitrap XL) as described previously (Lu et al., 2011; Wendrich et al., 2017). nLC-MSMS system quality was checked with PTXQC (Bielow et al., 2016) using the MaxQuant result files. LCMS data with all MS/MS spectra were analyzed with the MaxQuant quantitative proteomics software package (Cox et al., 2014) as described before (Smaczniak et al., 2012; Wendrich et al., 2017). A protein database with the protein sequences of *L. monocytogenes* LO28 (accession: PRJNA664298) was downloaded from NCBI (www.ncbi.nlm.nih.gov). Filtering and further bioinformatics and statistical analysis of the MaxQuant ProteinGroups file was performed with Perseus (Tyanova et al., 2016). Reverse hits and contaminants were filtered out. Protein groups were filtered to contain minimally two peptides for protein identification of which at least one is unique and at least one is unmodified. Also, each comparison (WT versus variants) required at least three valid values in either WT or variant. Data visualization was performed using the statistical programming language R (version 3.6.0). Significant up- or downregulation was defined as a change in abundance relative to the WT of at least 10 times (1 log), with an adjusted negative log *p*-value smaller than 0.01.

2.7. Whole genome sequencing and SNP analysis

Genomic DNA of *L. monocytogenes* LO28 WT strain for PacBio sequencing was isolated using the DNeasy Blood and tissue kit (Qiagen, Hilden, Germany). Two times 2 mL of overnight culture was pelleted at 17,000 ×*g*. The pellets were washed with 1 mL PPS and resuspended in 1 mL lysis buffer (20 mM Tris-HCl, 2 mM EDTA, 1.2% (*w/v*) Triton X-100, 20 mg/mL lysozyme, pH 8.0). The suspension was incubated at 37 °C for 1 h under gentle shaking in an Eppendorf Thermomixer 5436 (Eppendorf AG, Hamburg, Germany). Subsequently 10 µL of RNAse 20 mg/mL (Qiagen, Hilden, Germany) was added and incubated for 5 min at room temperature, after which 62.5 µL proteinase K and 500 µL AL buffer (provided by the manufacturer) were added. After incubation at 56 °C for 1 h under gentle shaking, 500 µL absolute ethanol was added. The suspension was transferred to a spin column provided by the kit and incubated for 10 min to allow for maximal binding of DNA. The columns were centrifuged for one minute at 6000 ×*g*. The filters were subsequently washed two times with 500 µL of buffer AW1 (provided by the manufacturer) at 6000 ×*g*, and two times with 500 µL of buffer AW2 (provided by the manufacturer). To remove any trace of buffer the columns were centrifuged at 17,000 ×*g* for 3 min. Subsequently, 53 µL of AE buffer was added to the centre of the column and incubated for 10 min before centrifugation at 6000 ×*g*. Samples were stored at 4 °C until sequencing.

PacBio sequencing was performed by Eurofins GATC (Eurofins GATC Biotech GmbH.

Germany) using a PacBio RS II system (Pacific Biosystems) resulting in 80,017 reads pre-filtering, with a N50 of 16,970 bp. Read correction, trimming, and de-novo assembly were performed in Canu V1.8 (Koren et al., 2017) running on a 2018 MacBook Pro under MacOS Mojave Version 10.14.3. Overhangs were trimmed using Circlator (Hunt et al., 2015) resulting in a 2,975,254 bp linear genome with *dnaA* as the first

gene. Error correction was done using Pilon version 1.123 with Illumina reads obtained previously (Metselaar et al., 2015). The resulting sequence and raw reads were submitted to GenBank and the sequence read archive respectively (at www.ncbi.nlm.nih.gov) with accession: PRJNA664298.

Strains used and Evolved variants 15EV1 and 15EV2 obtained in the evolution experiment were grown in 9 ml BHI tubes (Oxoid) for 18 ± 2 h at 37 °C. In total 1.8 mL of the culture was centrifuged for 5 min at 13,000 rpm to obtain a cell pellet. After removal of the supernatant the cell pellet was resuspended and stored in 450 µL DNA/RNA Shield (Zymo Research) at 4 °C until DNA extraction. The DNA was extracted by BaseClear (Leiden, the Netherlands) and paired-end 2 × 150 bp short-reads were generated using a Nextera XT library preparation (Illumina). The paired-end reads were sequenced on a NovaSeq 6000 system (Illumina). Raw reads were trimmed and de novo assembled using CLC Genomics Workbench v 10.0 (Qiagen, Hilden, Germany). SNP analysis of evolved variants against the LO28 WT reference was performed using SNIPPY 3.2 (Seemann, 2015) and Pilon using the "--changes" argument (Walker et al., 2014).

2.8. Mutant construction

Mutants (Table 1) were constructed using the temperature sensitive suicide plasmid pAULA (Chakraborty et al., 1992). The *rpsU* gene from either variant 15, 15EV1, or 15EV2 was amplified from gDNA by KAPA HiFi Hotstart ReadyMix (KAPA Biosystems, USA), using the primers listed in Supplementary Table S1. The resulting fragments were ligated in frame to the pAULA multiple cloning site via EcoR1 and Sal1 restriction that were introduced to the fragments by the respective primers.

The resulting plasmid was electroporated (2.5 kV, 25 µF, 200 Ω), in a 0.2 cm cuvette using a BIO-RAD GenePulser, to the appropriate *L. monocytogenes* cells, and plated on BHI agar at 30 °C with 5 µg/mL erythromycin to select for transformants.

Two erythromycin resistant colonies per construct were inoculated in separate tubes in BHI broth supplemented with 5 µg/mL erythromycin and grown overnight at 42 °C to select for plasmid integration. Selected strains resulting from a single cross-over integration event were grown overnight in BHI at 30 °C to induce double crossover events and were subsequently plated at 30 °C. Resulting colonies were replica plated on BHI with and without 5 µg/mL erythromycin and incubated at 30 °C. Colonies sensitive to erythromycin were selected. PCR using the primers listed in Supplementary Table S1 and DNA sequencing (BaseClear B.V. Leiden, The Netherlands) of erythromycin sensitive colonies confirmed the correct point mutation in the respective genes and the lack of additional mutations in the targeted region.
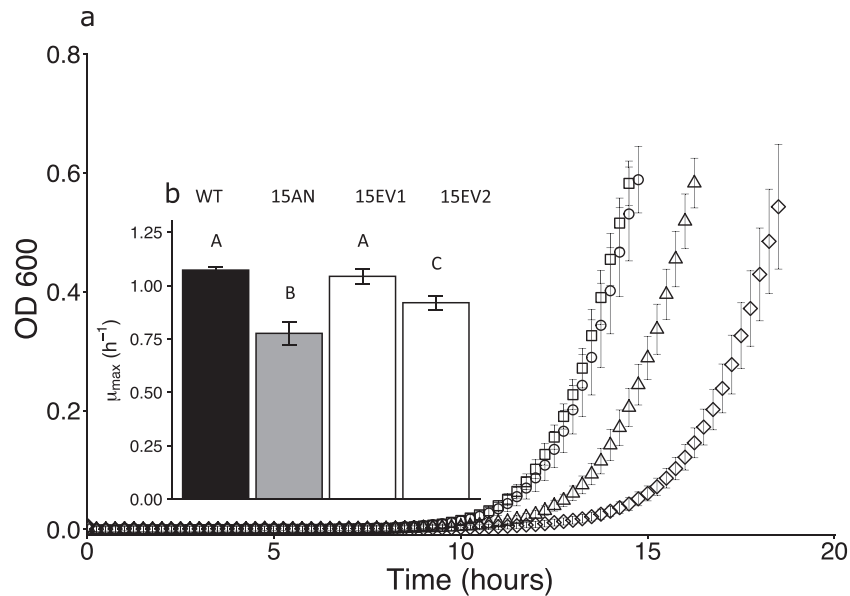
2.9. Statistical testing

Hypothesis testing was performed in the statistical programming language R (version 3.6.0) using the t.test() and var.test() functions.
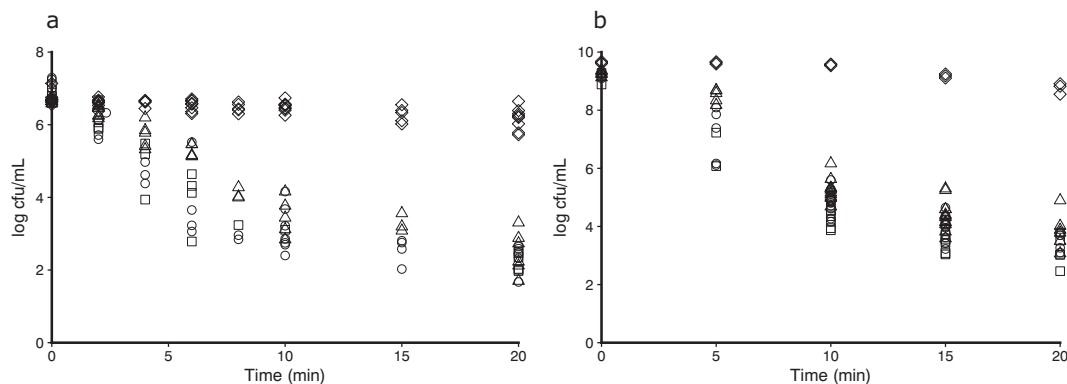
3. Results

3.1. Growth kinetics of evolved variants

The experimental evolution regime resulted in the selection of two

Fig. 1. Growth performance of *L. monocytogenes* LO28 WT, variant 15, 15EV1, and 15EV2 (a) growth curves for LO28 WT (squares), variant 15 (diamonds), 15EV1 (circles), and 15EV2 (triangles), (b) Maximum specific growth rates (μ_{max}) for *L. monocytogenes* LO28 WT, variant 15, 15EV1, and 15EV2. Different capital letters show statistically significant differences.

Fig. 2. Survival of *L. monocytogenes* LO28 WT, variant 15, 15EV1, and 15EV2 after exposure to heat (55 °C) (a) or acid stress (pH 3.0) (b). The wild type is represented by squares, variant 15 by diamonds, and variants 15EV1 and 15EV2, are represented by circles and triangles respectively.

evolved variants, Evolved 1 and Evolved 2 (15EV1 and 15EV2, respectively). The growth kinetics of evolved variants 15EV1 and 15EV2 were assessed (Fig. 1a) and showed that the experimental evolution regime had successfully selected for evolved variants after 16 and 18 daily transfers (~105 and ~120 generations), that showed increased μ_{max} when compared to variant 15 (Fig. 1a). The μ_{max} of both evolved strains was significantly higher than that of variant 15 whereas the μ_{max} of 15EV1 was even not significantly different from the μ_{max} of the LO28 WT strain, while strain 15EV2 had a slightly lower μ_{max} (Fig. 1b).

### 3.2. Multiple-stress resistance of evolved variants

Since the evolved variants 15EV1 and 15EV2 showed increased fitness, we compared their resistance to heat stress (55 °C) and acid stress (pH 3.0) to that of variant 15 (Fig. 2). In the heat stress experiments (Fig. 2a), variant 15 started with approximately 6.8 log cfu/mL, and showed little inactivation after 20 min of exposure, with a concentration of around 6 log cfu/mL. In contrast, after 20 min of exposure the concentrations of both evolved variants 15EV1 and 15EV2 decreased and were not significantly different from the LO28 WT strain with concentrations of around 2.5 log cfu/mL ($p > 0.05$). For acid stress

experiments (Fig. 2b), variant 15 again only showed a small (<1 log cfu/mL) decrease in cell counts after 20 min, while both evolved variants and also the LO28 WT strain showed over 5 log cfu/mL reduction after 20 min. These data indicate that both evolved variants 15EV1 and 15EV2 have lost their resistance to heat stress and acid stress when compared to variant 15.

3.3. Proteomic analysis of variant 15, 15EV1, and 15EV2

Comparative gene profiling analysis of *L. monocytogenes* LO28 WT and variant 15, previously showed upregulation of 116 genes with a major contribution of general stress sigma factor SigB dependent regulon members in late-exponential phase cells grown in non-stressed conditions in BHI (Koomen et al., 2018).

Here, we investigated the proteomes of late-exponential phase cells of *L. monocytogenes* LO28 WT, variant 15 and evolved variants 15EV1 and 15EV2 (Fig. 3). Presenting the data compared to the WT shows significant differences for variant 15 (Fig. 3), in line with previously reported differences in gene expression profiles and phenotypes (Koomen et al., 2018). Notably, our proteomics analysis revealed that out of the 29 proteins annotated as belonging to the SigB regulon in this
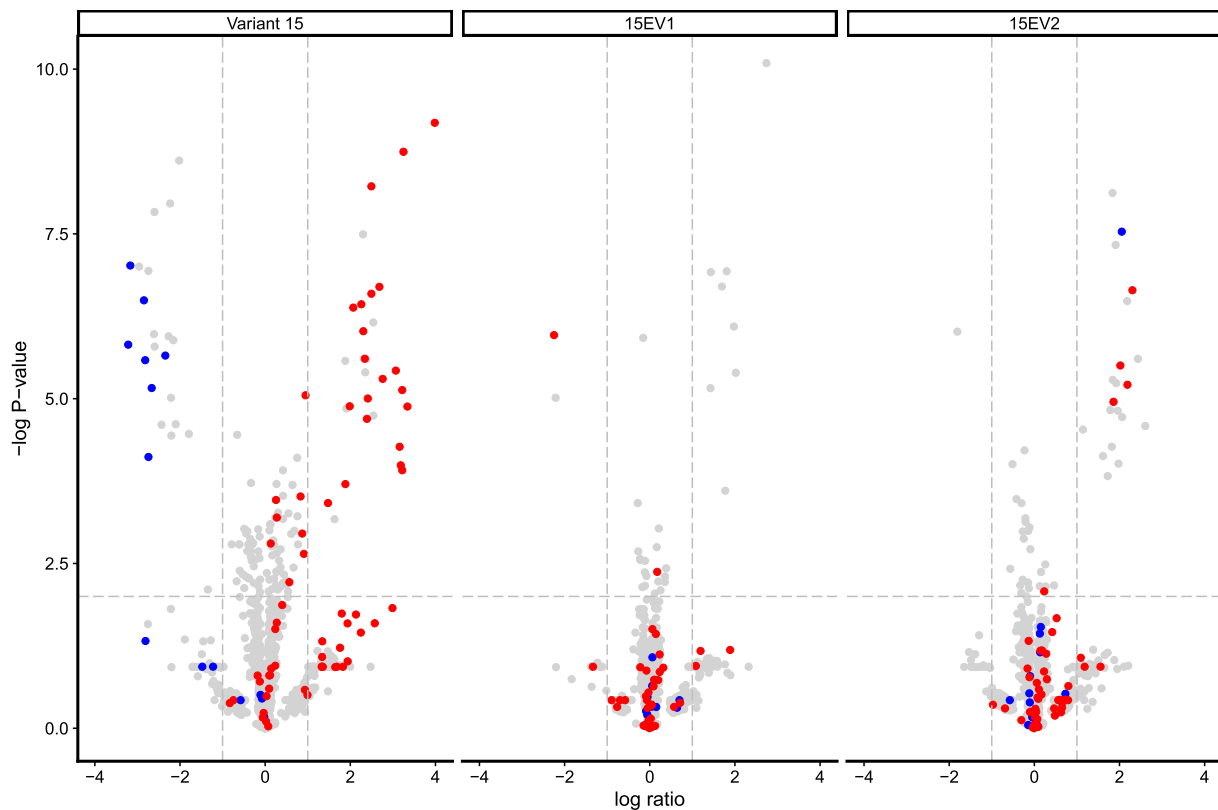
Fig. 3. Volcano plot of significantly differentially abundant proteins of *L. monocytogenes* variant 15, 15EV1, and 15EV2 compared to the wild type. The $-\log_{10}$ (Benjamini–Hochberg corrected *P* value) is plotted against the $\log_{10}$ (fold change: variant over WT). Horizontal dotted line represents the cutoff for $-\log_{10}$ (P), vertical dotted lines represent $\log_{10}$(fold change) cutoff. Red dots represent genes regulated by sigB, blue dots represent genes involved in the formation and regulation of flagella. The expression of individual proteins is listed in Supplementary Tables S2–S4. (For interpretation of the references to colour in this figure legend, the reader is referred to the web version of this article.)

sample, 21 were higher expressed in variant 15 compared to LO28 WT, (Fig. 3). These include stress resistance proteins such as OpuCA (lmo1428), OpuCC (lmo1426), and SepA (lmo2157) (Kazmierczak et al., 2003; Milohanic et al., 2003). For a full list, see Supplementary Table S1. In accordance with gene expression data, and the non-motile phenotype of variant 15 (Koomen et al., 2018), proteomics data show a significant reduced expression of motility and chemotaxis associated proteins such as MotA (lmo0685), MotB (lmo0686), CheA (lmo0692), and chemotaxis response regulator CheY (lmo0691). As anticipated, the proteomic profiles for 15EV1 and 15EV2 were more similar to that of the WT, and we found seven and twenty proteins expressed above the stringent threshold in 15EV1 and 15EV2, respectively (see Supplementary Tables S2 and S3). None of the genes that are upregulated in 15EV1 are part of the sigB regulon. Four of the upregulated proteins in 15EV2 were part of the SigB regulon, namely, succinate semialdehyde dehydrogenase (lmo0913), hypothetical protein lmo2748, opuCA (lmo1428), and the pyruvate oxidase lmo0722. The low relative abundance of SigB upregulated proteins matches the WT-like phenotypes of 15EV1 and 15EV2, including the higher fitness and loss of acid and heat stress resistance.

3.4. Whole genome sequencing of 15EV1 and 15EV2

Previous whole genome sequencing and Structural Variation (SV) analysis of *L. monocytogenes* LO28 WT and variant 15 revealed a Single Nucleotide Polymorphism (SNP) in the *rpsU* gene, coding for 30S ribosomal protein S21 (Metselaar et al., 2015). This SNP led to an arginine to proline substitution in the RpsU protein (denoted here as RpsU[17Arg-Pro]). Strikingly, whole genome sequencing and Structural Variation (SV) analysis of *L. monocytogenes* evolved variants 15EV1 and 15EV2

revealed a single SNP in the same codon of the *rpsU* gene, while no other SNPs were identified. In the *rpsU* gene of 15EV1 the Cytosine in position 50 mutated to Adenine, while in 15EV2 the Cytosine in position 49 mutated into Adenine, (see Table 2) resulting in amino acid changes from Proline (codon, CCT) to Histidine (codon, CAT) in 15EV1 (RpsU[17Pro-His]), and Threonine (codon, ACT) in 15EV2 (RpsU[17Pro-Thr]) (Fig. 4a, b). Since amino acid substitutions can disrupt protein structure, potentially altering protein stability or function, we analyzed the protein sequences of WT and variants using the online tool CFSSP (Ashok Kumar, 2013) Again, the protein structure of RpsU in WT and the evolved variants appeared similar, while an extra proline-associated turn was predicted in variant 15 (see Supplementary Fig. 1). The putative proline-induced turn may disrupt the RpsU[17Arg-Pro] protein structure as proline has been described as a helix breaker (Chou and Fasman, 1974), which might result in loss of functionality and/or exclusion from the 30S ribosome in variant 15.

3.5. Fitness and stress resistance of constructed mutants

To confirm the arginine to proline substitution at position 17 in *rpsU* as the mutation underlying the multiple-stress resistant phenotype of variant 15, we introduced RpsU[17Arg-Pro] into a *L. monocytogenes* LO28 WT background. Additionally, we also introduced the two SNP's that were selected by experimental evolution in 15EV1 and 15EV2, namely, RpsU[17Arg-His] and RpsU[17Agr-Thr]. Analysis of growth performance showed that the μ_{max} as proxy for fitness of the constructed RpsU[17Arg-Pro] mutant was similar to that of variant 15, and that of the constructed RpsU[17Arg-His] and RpsU[17Arg-Thr] mutants was similar to that of the corresponding evolved variants 15EV1 and 15EV2, respectively (Table S4). Subsequently, we tested the response of late exponential phase cells of the

Table 2
Mutations *in L. monocytogenes* variants found by WGS and SNP analysis.

Variant	Position	Strand	NT	AA	Locus tag	Product
15	1521940	−	50G > C	17R > P	IEJ01_07680	30S ribosomal protein S21
15EV1	1521940	−	50C > A	17P > H	IEJ01_07680	30S ribosomal protein S21
15EV2	1521939	−	49C > A	17P > T	IEJ01_07680	30S ribosomal protein S21

constructed mutants to heat (55 °C) stress (Fig. 5a) and acid (pH 3.0) stress (Fig. 5b). As expected, the LO28 WT strain with the introduced RpsU[17Arg-Pro] substitution showed significant ($p < 0.05$) higher heat and acid resistance after 10 min of treatment than the LO28 WT strains with the introduced RpsU[17Arg-His] and RpsU[17Arg-Thr] substitutions. These results confirmed that only the RpsU[17Arg-Pro] substitution results in the multiple-stress resistant phenotype typical of variant 15, while RpsU amino acid substitutions mimicking variants 15EV1 and 15EV2 results in WT like fitness and stress sensitive phenotypes.

To test whether RpsU, with a proline at position 17, could induce phenotypic switching in other *L. monocytogenes* strains, we also introduced the RpsU[17Arg-Pro] mutation into *L. monocytogenes* EGDe, which is one of the best studied strains of *L. monocytogenes* including its stress survival capacity (Becavin et al., 2014). Analysis of the growth

performance of EGDe WT and its RpsU[17Arg-Pro] mutant at 30 °C showed reduced fitness for the latter one, reflected in a lower μ_{max} (0.86 h^{-1} ± standard deviation 0.01 h^{-1}) compared to that of EGDe WT (1.10 h^{-1} ± standard deviation 0.02 h^{-1}) (Fig. 6). A comparative analysis previously showed that EGDe has a higher resistance to heat stress than LO28 (Aryani et al., 2015), and this was also reflected in the inactivation data shown in Fig. 7, where heat inactivation at 55 °C resulted in a decrease of about 2.5 log cfu/mL in 20 min for the EGDe WT (Fig. 7a). As expected, higher stress resistance was observed for the EGDe strain carrying the RpsU[17Arg-Pro] mutation, with stable cell counts maintained during the treatment time (Fig. 7a). We observed a similar trend when both strains were exposed to acid stress, with enhanced acid stress survival for the RpsU[17Arg-Pro] EGDe mutant strain (Fig. 7b). The combination of all results provides evidence that sequential mutations in *rpsU* resulting in RpsU[17Arg-Pro] and subsequently RpsU[17Pro-His] or RpsU[17Pro-Thr], enable a switch between low fitness/high stress resistance and high fitness-low stress resistance phenotypes in *L. monocytogenes*.

4. Discussion

Previous genotyping and phenotyping studies showed that the multiple-stress resistance of *L. monocytogenes* LO28 variant 15 with RpsU[17Arg-Pro] was linked to induction of the SigB regulon, and was correlated with reduced fitness (Koomen et al., 2018). Here, we have used experimental evolution to select for mutations in variant 15 that increased fitness.

The two evolved lines fixed two different mutations, leading to two
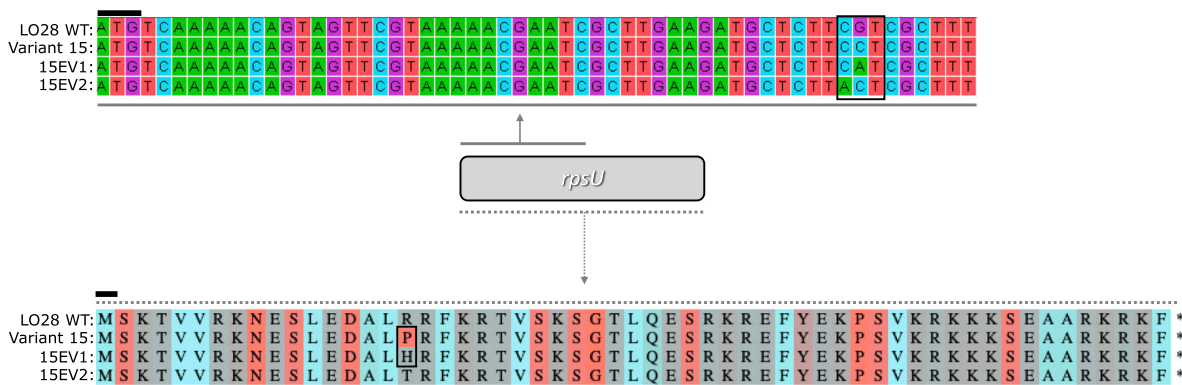
Fig. 4. Sequence alignment of *rpsU* (top) and amino acid sequence of RpsU in *L. monocytogenes* LO28 WT and variant 15 and 15EV1 and 15EV2. The upper alignment represents the nucleotide sequence of the region where mutations were found. The black line indicates the start codon of the *rpsU* gene. The lower alignment represents the amino acid sequence of the complete RpsU protein and the effect of the mutations on the amino acid sequence. Amino acids predicted to cause turns in the tertiary protein structure are shaded red, and amino acids at position 17 are boxed, including the extra turn in variant 15 caused by proline (P). (For interpretation of the references to colour in this figure legend, the reader is referred to the web version of this article.)
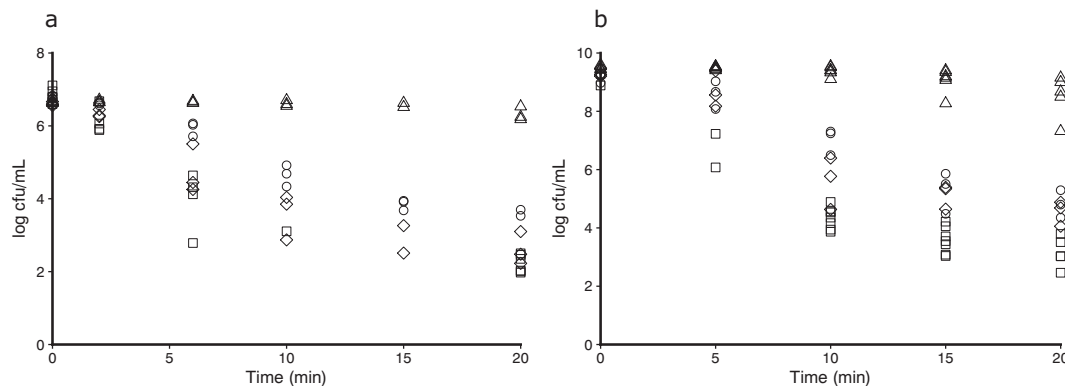
Fig. 5. Survival of *L. monocytogenes* LO28 WT, and constructed mutants, during heat (55 °C) (a) or acid (pH 3.0) (b) stress. LO28 WT is represented by squares, LO28 with RpsU[17Arg-Pro] is represented by triangles, LO28 with RpsU[17Arg-Thr], is represented by circles, and LO28 with RpsU[Arg17His] by diamonds.
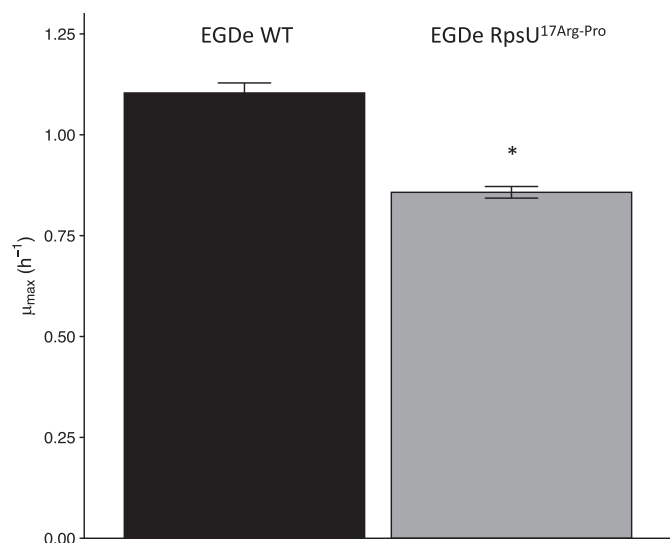
Fig. 6. Maximum specific growth rates (μ_{max}) for *L. monocytogenes* EGDe, and EGDe RpsU[17Arg-Pro]. Asterisk denotes significant difference.

different amino acid substitutions both at position 17 in RpsU, namely, RpsU[17Pro-His] (15EV1) and RpsU[17Pro-Thr] (15EV2) resulting in reversion to WT-like fitness (Fig. 1) and stress resistance (Fig. 2). The experimental evolution regime had successfully selected for evolved variants after 16 and 18 daily transfers (~105 and ~120 generations). We modelled the kinetics of the WT and variant 15 ancestor based on the μ_{max} reported by Metselaar et al. (2016) for the growing conditions that were used during experimental evolution. We used a 3-phase model based on Buchanan et al., 1997, with a logN$_{max}$ of 9.5 log cfu/mL, and took into account the Jameson effect (Jameson, 1962), that addresses growth suppression by the dominant strain in a multi strain population when the dominant strain reaches its stationary phase. We then estimated that after 6 rounds (~40 generations) one EV15 cell (with initial fraction $1 * 10^{-7.5}$) could have reached the same population density as the variant 15 strain, which is in line with the successful outcome of the experimental evolution experiment.

Random insertion of a proline residue is known to disrupt protein structure, potentially altering the stability or function of the protein (Chou and Fasman, 1974). Combined with data obtained with the constructed RpsU[17Arg-Pro], RpsU[17Arg-His], and RpsU[17Arg-Thr] mutants, we provided evidence that replacing the putative disruptive proline at position 17 in *L. monocytogenes* variant 15 with amino acids that do not have such strong disruptive effects, i.e., threonine or histidine, can restore WT-like functioning of the RpsU protein with an arginine at position 17. Although both evolved lines fixed a compensatory

mutation, they did not fix the same mutation, and we did not find a reversion to the original RpsU[17Arg]. Based on the slight difference in μ_{max} and proteomic profile between 15EV1 and 15EV2, we hypothesize that the RpsU[17Arg-His] mutation is slightly more efficient in restoring the WT phenotype than RpsU[17Arg-Thr].

The previously described variant 14 with a complete deletion of *rpsU* and variant 15 have highly comparable phenotypical behaviour (Koomen et al., 2018; Metselaar et al., 2015), which indicates that RpsU is not essential for growth, and that RpsU[17Arg-Pro] in variant 15 either lost its functionality, or is not (efficiently) incorporated into the 30S ribosome that together with the 50S ribosome constitutes the 70S ribosome. Notably, the additional introduction in the current study of the RpsU[17Arg-Pro] mutation in the well-studied *L. monocytogenes* EGDe strain, also resulted in a phenotypic switch from high fitness-low stress resistance to low fitness-high stress resistance (see Figs. 6 and 7), providing evidence that the observed changes in behaviour are strain independent and caused by a single arginine-proline substitution at position 17 in RpsU. Moreover, studies in *Bacillus subtilis*, a closely related firmicute, have also shown that RpsU was not essential for growth, but that deletion of the protein leads to altered phenotypes including loss of motility and a reduced growth rate (Akanuma et al., 2012).

Induction of multiple-stress resistance in *L. monocytogenes* by SigB is tightly controlled by the so-called stressosome, a protein complex that acts as a signal relay hub integrating multiple environmental (stress) signals (Guariglia-Oropeza et al., 2014; Impens et al., 2017). Activation of a large fraction of the SigB regulon during non-stress growth conditions in LO28 variant 15 and in LO28 carrying the RpsU[17Arg-Pro] mutations points to an (in)direct interaction between the 70S ribosome and the stress signalling cascade. How the presumed loss of function of the 30S RpsU[17Arg-Pro] variant protein affects functioning of the 70S ribosome resulting in reduced fitness and activation of the SigB regulon remains to be elucidated.

Previous studies describing performance of multiple-stress resistant variants in a model food chain considered the trade-off between increased stress resistance and lower fitness (Abee et al., 2016; Metselaar et al., 2015). The information that selection of multiple-stress resistant variants following a single lethal stress exposure, could be followed by subsequent evolution of variants with increased fitness and loss of the stress resistant phenotype, may point to an additional layer of complexity that can be included in these scenario analyses. Notably, translation of these population dynamics that are based on the generation and performance of *L. monocytogenes* variants following single-nucleotide substitutions (SNPs) to ecology along the food chain and more specifically (over)representation in persistent strains, is currently not supported by analysis of WGS data. Recently, Harrand et al. (2020) studied the evolution of *L. monocytogenes* persistence in a food processing plant over multiple years and genotyping of isolates showed limited single-nucleotide substitutions (SNPs), and a more prominent
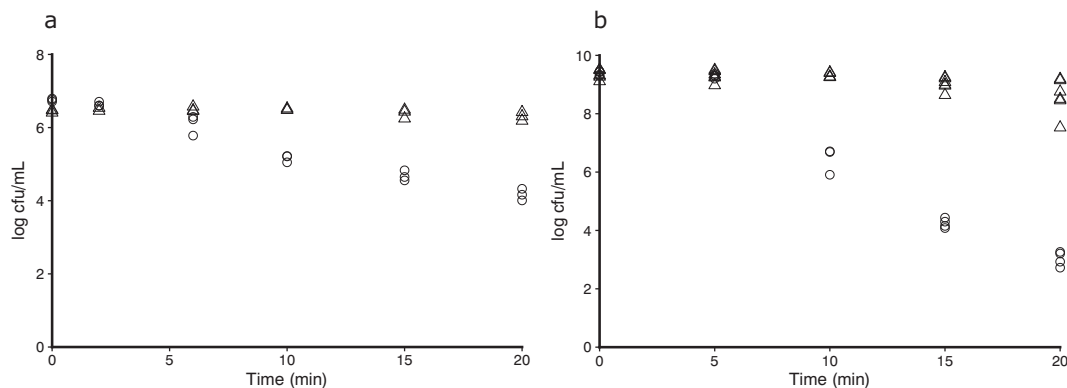
Fig. 7. Survival of *L. monocytogenes* EGDe wild type, and EGDe RpsU[17Arg-Pro], after exposure to heat (55 °C) (a) or acid (pH 3.0) stress (b). The EGDe WT is represented by circles, EGDe RpsU[17Arg-Pro] by triangles.

role in strain diversification by gain and loss of prophages. Further studies are required to determine whether the observed lack of (over) representation of SNPs in RpsU, and specifically those resulting in RpsU$^{17Arg-Pro}$, in sequenced *L. monocytogenes* isolates is caused by reduced fitness affecting performance of stress resistant variants in *L. monocytogenes* enrichments from food and food processing samples according to the ISO 11290-1:2017 method.

The experimental evolution setup used in the current study, combined with genotyping and phenotyping of the two evolved variants, and the construction of targeted mutants in *L. monocytogenes* LO28 and EGDe, provides evidence that single amino acid substitutions in RpsU enable *L. monocytogenes* to switch between high fitness-low stress resistance and low fitness-high stress resistance. The exact mechanism of SigB induction following RpsU$^{17Arg-Pro}$ substitution or RpsU deletion (Koomen et al., 2018; Metselaar et al., 2015) and the impact on 70S ribosome function and the stressosome-mediated signalling cascade is currently under investigation in our group. Ultimately, a better understanding of the processes involved will add to a further insight into factors contributing to strain diversity and population heterogeneity in *L. monocytogenes* stress sensing and survival capacity and its transmission in the food chain.

Supplementary data to this article can be found online at https://doi.org/10.1016/j.ijfoodmicro.2021.109269.

Declaration of competing interest

The authors declare that they have no known competing financial interests or personal relationships that could have appeared to influence the work reported in this paper.

References

Abee, T., Koomen, J., Metselaar, K.I., Zwietering, M.H., Besten, den H.M.W., 2016. Impact of pathogen population heterogeneity and stress-resistant variants on food safety. Annu. Rev. Food Sci. Technol. 7, 439–456. https://doi.org/10.1146/annurev-food-041715-033128.

Akanuma, G., Nanamiya, H., Natori, Y., Yano, K., Suzuki, S., Omata, S., Ishizuka, M., Sekine, Y., Kawamura, F., 2012. Inactivation of ribosomal protein genes in *Bacillus subtilis* reveals importance of each ribosomal protein for cell proliferation and cell differentiation. J. Bacteriol. 194, 6282–6291. https://doi.org/10.1128/JB.01544-12.

Aryani, D.C., Besten, den H.M.W., Hazeleger, W.C., Zwietering, M.H., 2015. Quantifying variability on thermal resistance of *Listeria monocytogenes*. Int. J. Food Microbiol. 193, 130–138. https://doi.org/10.1016/j.ijfoodmicro.2014.10.021.

Ashok Kumar, T., 2013. CFSSP: Chou and Fasman secondary structure prediction server. Wide Spectrum: Research Journal 1 (9), 15–19.

Becavin, C., Bouchier, C., Lechat, P., Archambaud, C., Creno, S., Gouin, E., Wu, Z., Kuhbacher, A., Brisse, S., Pucciarelli, M.G., Garcia-del Portillo, F., Hain, T., Portnoy, D.A., Chakraborty, T., Lecuit, M., Pizarro-Cerda, J., Moszer, I., Bierne, H., Cossart, P., 2014. Comparison of widely used *Listeria monocytogenes* strains EGD, 10403S, and EGD-e highlights genomic differences underlying variations in pathogenicity. mBio 5, 312–379. https://doi.org/10.1128/mBio.00969-14.

Bielow, C., Mastrobuoni, G., Kempa, S., 2016. Proteomics quality control: quality control software for MaxQuant results. J. Proteome Res. 15, 777–787. https://doi.org/10.1021/acs.jproteome.5b00780.

Biesta-Peters, E.G., Reij, M.W., Joosten, H., Gorris, L.G.M., Zwietering, M.H., 2010. Comparison of two optical-density-based methods and a plate count method for estimation of growth parameters of *Bacillus cereus*. Appl. Environ. Microbiol. 76, 1399–1405. https://doi.org/10.1128/AEM.02336-09.

Buchanan, R.L., Whiting, R.C., Damert, W.C., 1997. When is simple good enough: a comparison of the Gompertz, Baranyi, and three-phase linear models for fitting bacterial growth curves. Food Microbiol. 14, 313–326. https://doi.org/10.1006/fmic.1997.0125.

Chakraborty, T., Leimeister-Wächter, M., Domann, E., Hartl, M., Goebel, W., Nichterlein, T., Notermans, S., 1992. Coordinate regulation of virulence genes in *Listeria monocytogenes* requires the product of the *prfA* gene. J. Bacteriol. 174, 568–574. https://doi.org/10.1128/jb.174.2.568-574.1992.

Chou, P.Y., Fasman, G.D., 1974. Prediction of protein conformation. Biochemistry 13, 222–245. https://doi.org/10.1021/bi00699a002.

Cox, J., Hein, M.Y., Luber, C.A., Paron, I., Nagaraj, N., Mann, M., 2014. Accurate proteome-wide label-free quantification by delayed normalization and maximal peptide ratio extraction, termed MaxLFQ. Mol. Cell. Proteomics 13, 2513–2526. https://doi.org/10.1074/mcp.M113.031591.

Gollan, B., Grabe, G., Michaux, C., Helaine, S., 2019. Bacterial persisters and infection: past, present, and progressing. Annu. Rev. Microbiol. 73, 359–385. https://doi.org/10.1146/annurev-micro-020518-115650.

Guariglia-Oropeza, V., Orsi, R.H., Yu, H., Boor, K.J., Wiedmann, M., Guldimann, C., 2014. Regulatory network features in *Listeria monocytogenes*-changing the way we talk. Front. Cell. Infect. Microbiol. 4, 14. https://doi.org/10.3389/fcimb.2014.00014.

Guldimann, C., Boor, K.J., Wiedmann, M., Guariglia-Oropeza, V., 2016. Resilience in the face of uncertainty: sigma factor B fine-tunes gene expression to support homeostasis in gram-positive bacteria. Appl. Environ. Microbiol. 82, 4456–4469. https://doi.org/10.1128/AEM.00714-16.

Hunt, M., Silva, N.D., Otto, T.D., Parkhill, J., Keane, J.A., Harris, S.R., 2015. Circlator: automated circularization of genome assemblies using long sequencing reads. Genome Biol. 16, 294. https://doi.org/10.1186/s13059-015-0849-0.

Impens, F., Rolhion, N., Radoshevich, L., Bécavin, C., Duval, M., Mellin, J., del Portillo, F.G., Pucciarelli, M.G., Williams, A.H., Cossart, P., 2017. N-terminomics identifies Prli42 as a membrane miniprotein conserved in Firmicutes and critical for stressosome activation in *Listeria monocytogenes*. NAT. MICROBIOL 2, 1–13. https://doi.org/10.1038/nmicrobiol.2017.5.

Jameson, J., 1962. A discussion of the dynamics of *Salmonella* enrichment. Journal of Hygiene 60, 193–207.

Karatzas, K.A.G., Valdramidis, V.P., Wells-Bennik, M.H.J., 2005. Contingency locus in *ctsR* of *Listeria monocytogenes* Scott A: a strategy for occurrence of abundant piezotolerant isolates within clonal populations. Appl. Environ. Microbiol. 71, 8390–8396. https://doi.org/10.1128/AEM.71.12.8390-8396.2005.

Kazmierczak, M.J., Mithoe, S.C., Boor, K.J., Wiedmann, M., 2003. *Listeria monocytogenes* sigma B regulates stress response and virulence functions. J. Bacteriol. 185, 5722–5734. https://doi.org/10.1128/jb.185.19.5722-5734.2003.

Koomen, J., Besten, den H.M.W., Metselaar, K.I., Tempelaars, M.H., Wijnands, L.M., Zwietering, M.H., Abee, T., 2018. Gene profiling-based phenotyping for identification of cellular parameters that contribute to fitness, stress-tolerance and virulence of *Listeria monocytogenes* variants. Int. J. Food Microbiol. 283, 14–21. https://doi.org/10.1016/j.ijfoodmicro.2018.06.003.

Koren, S., Walenz, B.P., Berlin, K., Miller, J.R., Bergman, N.H., Phillippy, A.M., 2017. Canu: scalable and accurate long-read assembly via adaptive k-mer weighting and repeat separation. Genome Res. 27, 722–736. https://doi.org/10.1101/gr.215087.116.

Lecuit, M., 2007. Human listeriosis and animal models. Microbes Infect. 9, 1216–1225. https://doi.org/10.1016/j.micinf.2007.05.009.

Lu, J., Boeren, S., de Vries, S.C., van Valenberg, H.J.F., Vervoort, J., Hettinga, K., 2011. Filter-aided sample preparation with dimethyl labeling to identify and quantify milk fat globule membrane proteins. J. Proteome 75, 34–43. https://doi.org/10.1016/j.jprot.2011.07.031.

Metselaar, K.I., Besten, den H.M.W., Abee, T., Moezelaar, R., Zwietering, M.H., 2013. Isolation and quantification of highly acid resistant variants of *Listeria monocytogenes*. Int. J. Food Microbiol. 166, 508–514. https://doi.org/10.1016/j.ijfoodmicro.2013.08.011.

Metselaar, K.I., Besten, den H.M.W., Boekhorst, J., van Hijum, S.A.F.T., Zwietering, M.H., Abee, T., 2015. Diversity of acid stress resistant variants of *Listeria monocytogenes* and the potential role of ribosomal protein S21 encoded by *rpsU*. Front. Microbiol. 6, 422. https://doi.org/10.3389/fmicb.2015.00422.

Metselaar, K.I., Abee, T., Zwietering, M.H., Besten, den H.M.W., 2016. Modeling and validation of the ecological behavior of wild-type *Listeria monocytogenes* and stress-resistant variants. Appl. Environ. Microbiol. 82, 5389–5401. https://doi.org/10.1128/AEM.00442-16.

Milohanic, E., Glaser, P., Coppée, J.-Y., Frangeul, L., Vega, Y., Vázquez-Boland, J.A., Kunst, F., Cossart, P., Buchrieser, C., 2003. Transcriptome analysis of *Listeria monocytogenes* identifies three groups of genes differently regulated by PrfA. Mol. Microbiol. 47, 1613–1625. https://doi.org/10.1046/j.1365-2958.2003.03413.x.

NicAogáin, K., O`Byrne, C.P., 2016. The role of stress and stress adaptations in determining the fate of the bacterial pathogen *Listeria monocytogenes* in the food chain. Front. Microbiol. 7, 1916–1962. https://doi.org/10.3389/fmicb.2016.01865.

Radoshevich, L., Cossart, P., 2018. *Listeria monocytogenes*: towards a complete picture of its physiology and pathogenesis. Nat. Rev. Microbiol. 16, 32–46. https://doi.org/10.1038/nrmicro.2017.126.

Seemann, T., 2015. Snippy: fast bacterial variant calling from NGS reads. https://github.com/tseemann/snippy.

Smaczniak, C., Immink, R.G.H., Muiño, J.M., Blanvillain, R., Busscher, M., Busscher-Lange, J., Dinh, Q.D.P., Liu, S., Westphal, A.H., Boeren, S., Parcy, F., Xu, L., Carles, C.C., Angenent, G.C., Kaufmann, K., 2012. Characterization of MADS-domain transcription factor complexes in *Arabidopsis* flower development. Proc. Natl. Acad. Sci. U. S. A. 109, 1560–1565. https://doi.org/10.1073/pnas.1112871109.

Tyanova, S., Temu, T., Sinitcyn, P., Carlson, A., Hein, M.Y., Geiger, T., Mann, M., Cox, J., 2016. The Perseus computational platform for comprehensive analysis of (prote) omics data. Nat. Methods 13, 731–740. https://doi.org/10.1038/nmeth.3901.

Van Boeijen, I.K.H., Moezelaar, R., Abee, T., Zwietering, M.H., 2008. Inactivation kinetics of three *Listeria monocytogenes* strains under high hydrostatic pressure. J. Food Prot. 71, 2007–2013. https://doi.org/10.4315/0362-028x-71.10.2007.

Vázquez-Boland, J.A., Kuhn, M., Berche, P., Chakraborty, T., Domínguez-Bernal, G., Goebel, W., González-Zorn, B., Wehland, J., Kreft, J., 2001. *Listeria* pathogenesis and molecular virulence determinants. Clin. Microbiol. Rev. 14, 584–640. https://doi.org/10.1128/CMR.14.3.584-640.2001.

Walker, B.J., Abeel, T., Shea, T., Priest, M., Abouelliel, A., Sakthikumar, S., Cuomo, C.A., Zeng, Q., Wortman, J., Young, S.K., Earl, A.M., 2014. Pilon: an integrated tool for comprehensive microbial variant detection and genome assembly improvement. PLoS One 9, e112963. https://doi.org/10.1371/journal.pone.0112963.

Wendrich, J.R., Boeren, S., Möller, B.K., Weijers, D., De Rybel, B., 2017. In vivo identification of plant protein complexes using IP-MS/MS. Methods Mol. Biol. 1497, 147–158. https://doi.org/10.1007/978-1-4939-6469-7_14.

Wiśniewski, J.R., Zougman, A., Nagaraj, N., Mann, M., 2009. Universal sample preparation method for proteome analysis. Nat. Methods 6, 359–362. https://doi.org/10.1038/nmeth.1322.